ELSEVIER

Physica C 338 (2000) 179–188

PHYSICA C

www.elsevier.nl/locate/physc

Vortex dynamics in 2*H*-$NbSe_2$ containing striped regions of columnar defects

M.-O. André [a,1], M. Polichetti [a,b,*], H. Pastoriza [a,2], P.H. Kes [a]

[a] *Kamerlingh Onnes Laboratorium, Rijksuniversiteit Leiden, Postbus 9504, 2300 RA Leiden, The Netherlands*
[b] *Universitá degli Studi di Salerno, Dipartimento di Fisica, Istituto Nazionale di Fisica della Materia (INFM), Unitá di Salerno, Via S. Allende, 84081 Baronissi, Salerno, Italy*

Received 14 December 1999; received in revised form 30 March 2000; accepted 12 April 2000

Abstract

We have measured the resistivity and magnetic AC susceptibility of 2*H*-$NbSe_2$ single crystals containing alternating stripes of irradiated and non-irradiated regions of columnar defects created by heavy-ion bombardment. Without applied magnetic field, the sample undergoes a double-step transition into the superconducting state, each step corresponding to the transitions in the irradiated and non-irradiated regions, respectively. For fields smaller than half of the matching field and upon increasing the temperature, the onset of flux motion in the non-irradiated channels occurs, when the applied stress due to the electrical current equals the shear stress at the channel edges, while depinning in the irradiated stripes occurs at higher temperature. The weak amplitude dependence of the shear process suggests that it takes place at the melting transition. We observed only a single-step transition at DC magnetic fields larger than half the matching field, because pinning by the columnar defects in the irradiated stripes is much less effective, and consequently the shear stress at the channel edges is strongly reduced. The comparison between the shear stress deduced from *I–V* curves and the theoretical value $\tau_{max} = AC_{66}$ yields a value for the constant *A*, which is in good agreement with theoretical predictions.

PACS: 74.60.Ge; 74.25.Fy; 74.25.Ha
Keywords: Flux-line lattice dynamics; AC Susceptibility and transport properties; Type-II superconductors; Mixed state; $NbSe_2$

1. Introduction

Since the discovery of high-T_c superconductors, there has been great interest in the thermodynamic phase diagram of the ''vortex matter''. Several new vortex phases and transitions between them have been suggested theoretically with the support of experimental results (see for example Refs. [1–9], and references therein). Three aspects are responsible of the richness of the vortex phase diagram: quenched

* Corresponding author. Massimiliano Polichetti, Department of Physics, University of Salerno-INFM-84081 Baronissi (SA), Italy. Tel.: +39-89-965-360, +39-89-965-277; fax: +39-89-953-804.
E-mail address: polimax@sa.infn.it (M. Polichetti).
[1] Present address: Moving Magnet Technologies, Rue Christiaan Huyghens, 25000 Besancon, France.
[2] Present address: Centro Atómico Bariloche, Comisión Nacional de Energía Atómica, 8400 San Carlos de Bariloche, Argentina.

0921-4534/00/$ - see front matter
PII: S0921-4534(00)00302-6

disorder, anisotropy in the electronic properties, and thermal fluctuations. The $2H$-$NbSe_2$ represents a good candidate to study the influence of each of this aspects in the phase diagram: thermal fluctuations are reduced, due to the low T_c of this material, the anisotropy is close to that of the less anisotropic High-T_c superconductors, and finally it is one of the cleanest superconducting systems as revealed by the very low ratio between the critical current density (j_c) and the depairing current density (j_0). In fact, in the $2H$-$NbSe_2$ this ratio $j_c/j_0 = 10^{-5}$–10^{-6}, while in high-T_c superconductors $j_c/j_0 = 10^{-3}$–10^{-2}; in particular this very low ratio makes the $2H$-$NbSe_2$ an ideal system for the study of phase transitions. The dependence of the critical current density on temperature and DC magnetic field exhibits a peak [10,11], which can be explained using the Larkin–Ovchinnikov collective pinning theory [12]. Some authors have ascribed the peak to a melting transition [11,13], while others have attributed it to a crossover in the flow regime of the vortices [14].

In this paper, we present transport measurements which directly probe the shear strength of the vortex ensemble in $2H$-NbSe. The sample consists of a periodic structure of stripes with columnar defects introduced by high-energy ion bombardment, separated by non-irradiated channels. The columnar defects are cylindrical tracks of amorphous material with lateral size of the order of the coherence length. Although the effect is not as dramatic as in high-T_c superconductors, the columnar defects enhance the pinning properties of $2H$-$NbSe_2$ [15], for fields smaller than half of the dose-equivalent field [16–19] (the dose-equivalent or matching field is the field at which the vortex density equals the density of columnar defects).

With the field parallel and the current perpendicular to the walls of the channels, a Lorentz force directed parallel to the channels is exerted on the vortices. The onset of vortex flow in the channels occurs when the Lorentz force equals the shear force at the channel walls, which is exerted by the ensemble of pinned vortices in the stripes containing columnar defects. The current necessary to counterbalance the shear force (shear current) is given by the relationship [20]:

$$j_s = 2\tau_{max}/WB, \tag{1}$$

where B is the magnetic field, $\tau_{max} = AC_{66}$ is the flow stress, C_{66} is the shear modulus of the lattice which, at low fields, is given by

$$C_{66} = \frac{\Phi_0 B(1 - T/T_c)}{16\pi\mu_0 \lambda_{ab}^2(0)}. \tag{2}$$

A is a constant related to the anharmonicity in the lattice potential and to the dispersion of C_{66} and has values between $1/(2\pi)$ and $1/30$ [21,22], and W is the effective width of the channels (approx. 3 μm). Measurements in similar configurations have yielded relevant information on the vortex flow regimes of two-dimensional low-T_c superconductors, [23] and have also confirmed the melting scenario in $Bi_2Sr_2CaCu_2O_{8+x}$ (Bi-2212) [24]. The results presented in this paper reveal a double-step transition probed by resistivity and magnetic AC susceptibility at low-DC magnetic fields, i.e. lower than approximately half of the dose-equivalent field. The double-step transition observed in zero-field measurements can be attributed to the existence of two phases in the compound: the non-irradiated channels showing the same critical temperature as pristine samples, and the irradiated fraction of the sample with a slightly higher T_c, which may result from the destruction of the charge–density wave. At low DC magnetic fields, the double-step transition is due to the onset of vortex flow in the channels, when the applied current equals the shear current, followed by

Fig. 1. (a) Temperature dependence of the voltage for $j = 7.7 \cdot 10^4$ A/m^2, at DC field of 0 (△), 0.02 (▲), 0.04 (○), 0.06 (●), 0.08 (◇), 0.1 (■) T. An arrow indicates a zero-field measurement on a fully irradiated sample (◆). A second arrow indicates the kink in the $V(T)$ curve measured on the sample with the channel structure. The inset shows the same measurements but at the fields 0.5 (◆), 0.7 (○), and 1 (□) T (here the voltage scale is not necessary and, for simplicity, it is not reported). (b) Field dependence of the voltage for $j = 7.7 \cdot 10^4$ A/m^2 at different temperatures: 6.3 K(■), 6.5 K(○), 6.8 K(●), and 6.9 K(□).

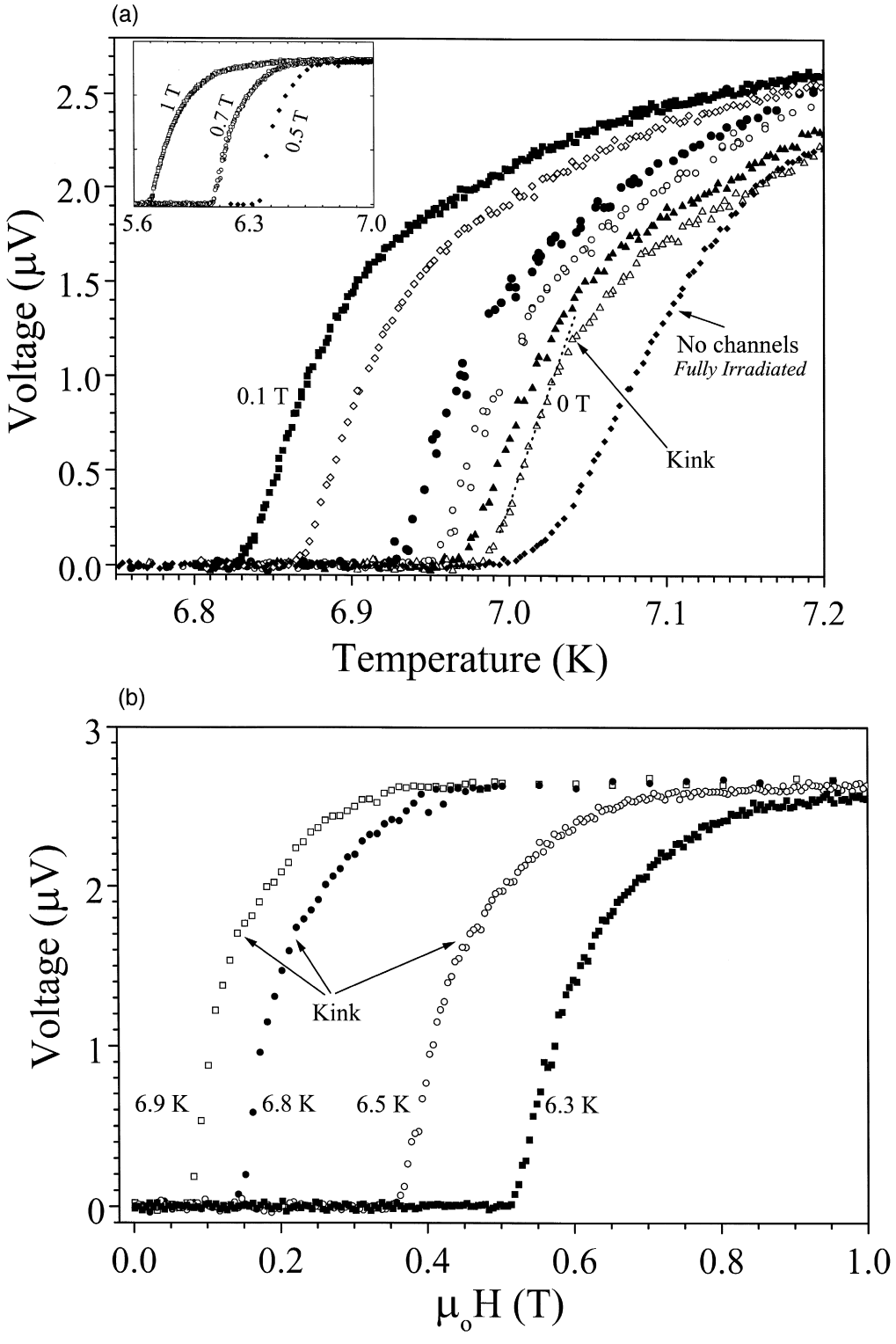
(a)
Voltage (μV)
Temperature (K)
1 T
0.7 T
0.5 T
0.1 T
0 T
No channels
Fully Irradiated
Kink
(b)
Voltage (μV)
μ0H (T)
Kink
6.9 K
6.8 K
6.5 K
6.3 K

depinning from the columnar defects at higher temperature. At DC magnetic fields larger than half the matching field, the efficiency of pinning by the columnar defects is strongly reduced, because of the excess vortices with respect to the available pinning tracks. The transition occurs only in a single-step, which indicates that the vortex motion is relatively homogeneous throughout the sample.

2. Experimental

We irradiated single crystals of 2*H*-$NbSe_2$ with 5.9 GeV ^{208}Pb ions at GANIL (Caen, France), according to the procedure described in Ref. [24]. The channel structure was obtained by covering the samples with a mask (see Ref. [24] for the details of the design and fabrication of the mask). The ion bombardment fluence was 5×10^{10} ions/cm^2 corresponding to a dose-equivalent field of 1 T. In order to verify the presence of the desired channel structure in the samples, the mica strips used as sample holders during the irradiation were cleaved, etched in a 40% solution of hydrofluoric acid and then investigated by polarised-light microscopy [24]. The morphology of the channel structure is similar to that of Ref. [24], i.e. the average width of the channels is approx. 3 μm, and the average distance between them is approx. 12 μm. The sample dimensions are $3 \times 0.5 \times 0.026$ mm^3. We measured the resistivity in the standard four-point configuration with a spacing between the voltage contacts of approximately 1 mm. In the resistivity measurements the current has been applied perpendicular to the channels walls, while the magnetic field direction is perpendicular to the sample (i.e. parallel to the channels walls); in this way the Lorentz force on the flux lines is exerted along the direction of the channels. The AC magnetic susceptibility measurements have been performed by using a non-commercial three-coil susceptometer in the bridge configuration, in which a lock-in amplifier measured the voltage induced in the two pick-up coils connected in series and wrapped in the opposite direction.

3. Results

In Fig. 1a, we present measurements of the DC resistivity as a function of temperature at various DC magnetic fields and using a current density $j = 7.7 \times 10^4$ A/m^2. Measurements as a function of the DC magnetic field at several temperatures are displayed in Fig. 1b. In both sets of measurements, the resistivity displays a characteristic kink indicated by arrows in the figures. Below the kink, the resistivity decreases linearly as a function of DC magnetic field and temperature, whereas between the kink and the normal-state resistivity, it is non-linear. The kink disappears at higher magnetic fields in Fig. 1a (see measurements in the inset), or lower temperatures in Fig. 1b. A fully irradiated sample from the same batch shows no kink, but a smooth transition, as shown in Fig. 1a.

We also measured the AC magnetic susceptibility of the sample showing the kink in resistivity. The AC susceptibility as a function of the DC magnetic field strongly depends on the temperature (Fig. 2a). At temperatures close to T_c, the imaginary part (χ'') exhibits a double-peak structure associated to a double-step transition in the real part (inset to Fig. 2a). As the temperature is decreased, the double-peak structure evolves into a single-peak in χ'' (see for instance the measurement at 6.3 K). Similarly, the double-step transition in the real part becomes a single-step transition as the temperature is decreased. Measurements as a function of temperature show the same behaviour: double-peak structure at low fields

Fig. 2. (a) Imaginary part (χ'') of the AC susceptibility as a function of the DC magnetic field at the same temperatures as in Fig. 1(b). The AC field amplitude and frequency are $h_{AC} = 0.5$ Oe and $\nu = 1300$ Hz respectively. The inset shows the behaviour of the real part (χ') of the AC susceptibility at $T = 6.85$ K. Notice the double step transition and the criterion used to determine the lines $S_1 = H_{c2,\mathrm{chan}}$ (1st Trans.) and $S_2 = H_{c2,\mathrm{chan}}$ (2nd Trans.) in Fig. 4. (b) Temperature dependence of the imaginary part of the AC susceptibility at the DC field 0 (△), 0.1 (■), 0.5 (♦), 0.7 (○), 1 (□) T, $h_{AC} = 0.5$ Oe and $\nu = 1300$ Hz.

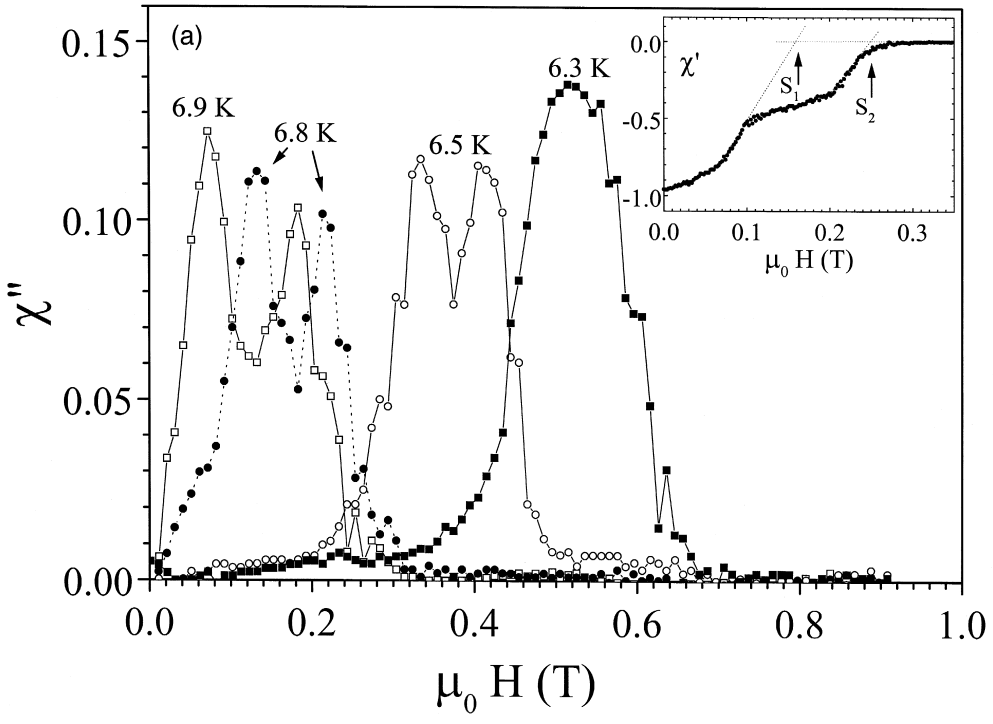
(a)
6.9 K
6.8 K
6.5 K
6.3 K
χ''
μ0 H (T)
χ'
S1
S2
μ0 H (T)

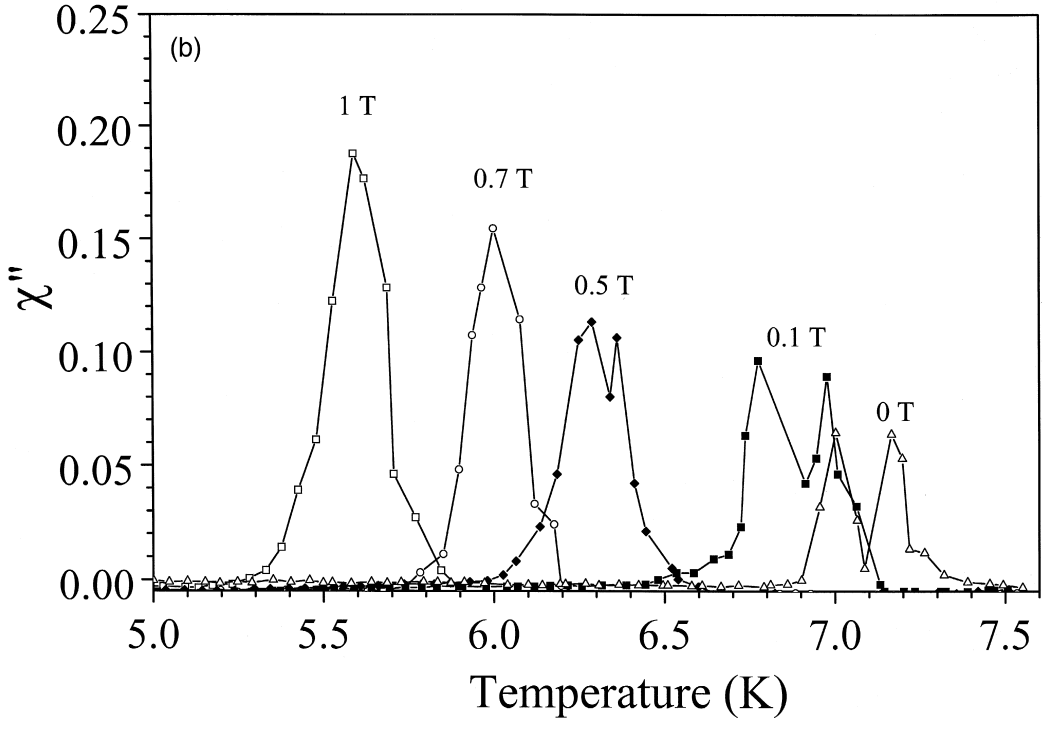
(b)
1 T
0.7 T
0.5 T
0.1 T
0 T
χ''
Temperature (K)

evolving towards a single-peak structure as the DC magnetic field is increased (Fig. 2b). The position of both peaks depends on the AC magnetic field amplitude (Fig. 3), with a more pronounced dependence for the peak at higher DC magnetic field. Both peaks become indistinguishable as the amplitude of the AC field is increased. The dependence of the AC susceptibility on the amplitude of the AC field is a signature of irreversible mechanisms, which may be governed either by bulk pinning or by a surface or geometrical barrier against the entry of vortices [25]. It is well established that above 50 G and in the perpendicular geometry ($H_{DC} \parallel c$), the major mechanism giving rise to magnetic irreversibility is bulk pinning [10,13,26], whereas below 50 G, the geometrical barrier becomes the dominant mechanism [27]. Therefore, we believe that the measurements presented in this paper bear the signature of bulk pinning irreversibility.

Some of the characteristic features observed on the different curves plotted in the previous figures are shown in the H–T diagram of Fig. 4. Two boundaries can be defined from the AC susceptibility data at low DC fields and high temperatures (Fig. 2) by the intercepts S_1 and S_2 of the line $\chi' = 0$ with the tangent to each step in measurements of χ' (see inset to Fig. 2a). The two lines correspond to measurements performed at the AC field amplitude $h_{AC} = 0.5$ Oe. One more line is that of H_{c2} measured in non-irradiated 2H-$NbSe_2$ samples of the same batch (such as those studied in Ref. [28]). The two additional lines are defined as the onset and the kink in resistivity (R_0 and R_{kink}, respectively), measured at the current density $j = 7.7 \cdot 10^4$ A/m^2.

An inspection of the H–T diagram immediately yields three observations. The line formed by the data points S_1 coincides with that of the upper critical field H_{c2} of non-irradiated samples, whereas

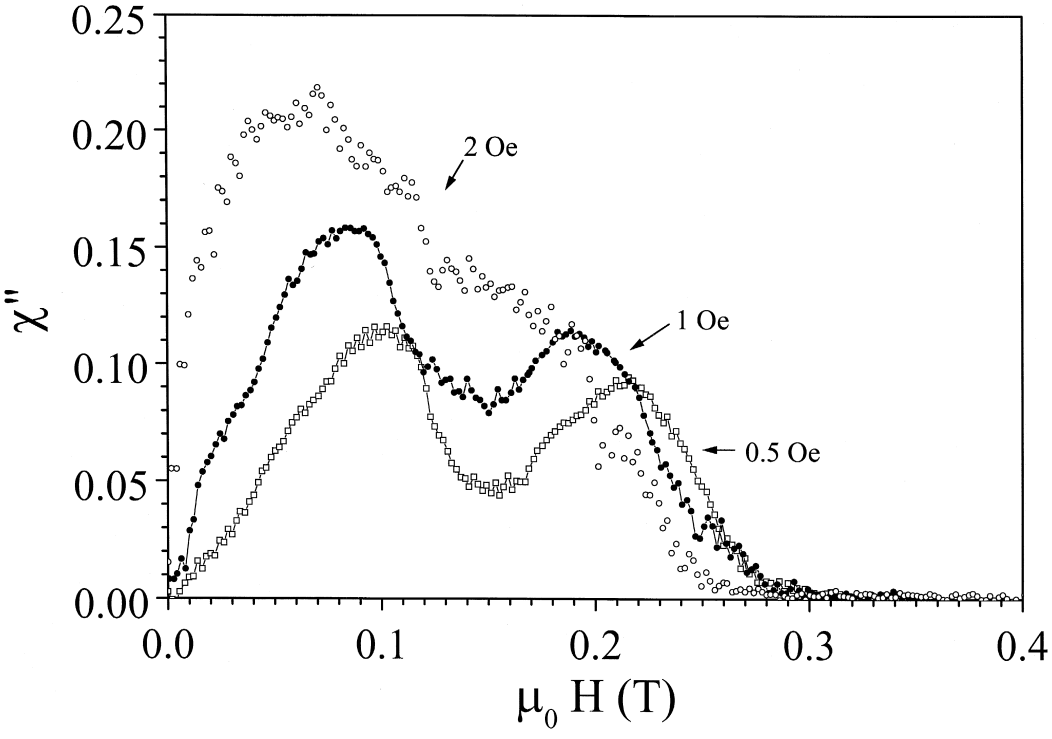

Fig. 3. Field dependence of the imaginary part of the AC susceptibility at different AC field amplitudes $h_{AC} = 0.5$ (□), 1 (●), and 2 (○) Oe at $T = 6.85$ K and $\nu = 1300$ Hz.

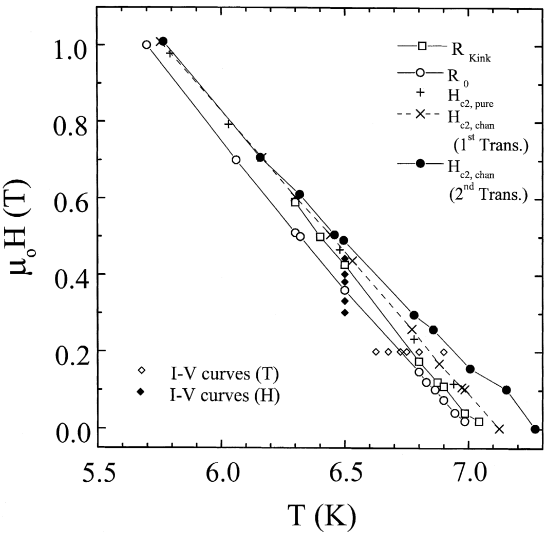

Fig. 4. $H-T$ plot showing the points corresponding to the kink (□, R_{kink}) and the onset (○, R_0) in resistivity measurements, H_{c2} of the non irradiated 2H-$NbSe_2$ sample (+, $H_{c2,\text{pure}}$), H_{c2} measured on the sample with channels (×, $S_1 \equiv H_{c2,\text{chan}}$ (1st trans.); ●, $S_2 \equiv H_{c2,\text{chan}}$ (2nd trans.)), and the points at which the $I-V$ curves have been measured. The lines are a guide to the eye.

the line S_2 tends to merge with the two latter ones at approximately 0.6 T.

In order to better characterise the different portions of the $H-T$ diagram delimited by these boundaries, we have measured several $I-V$ curves (Fig. 5) indicated by the vertical column of symbols at 6.5 K and the horizontal row of symbols at 0.2 T in Fig. 4. At fields and temperatures below the R_0 line, the $I-V$ curves are strongly non-linear, while the linearity is recovered above the R_{kink} line. In the intermediate region, the non-linearity follows a power-law with an exponent gradually approaching unity for the curves measured increasingly close to the R_{kink} line.

4. Discussion

Before analysing the $H-T$ diagram in more detail, an important task is the choice of a suitable criterion for the determination of H_{c2}. A criterion which is often used is the intercept of the line $\chi' = 0$

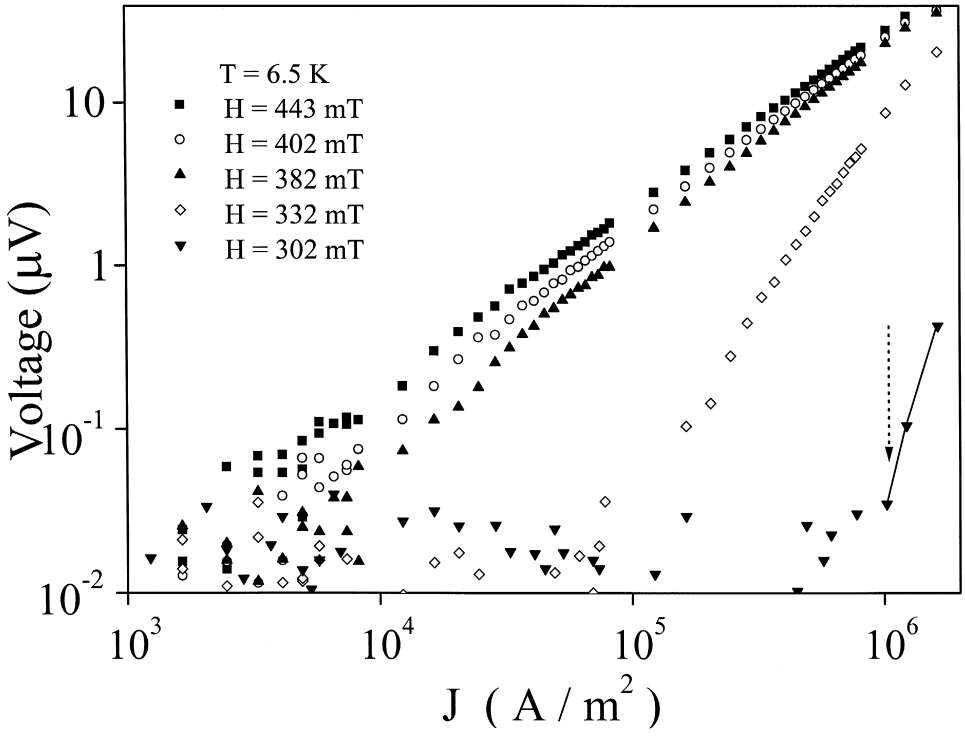

Fig. 5. $I-V$ characteristics measured at 6.5 K and at different DC fields. The arrow indicates the onset of resistance corresponding to the de-shearing of the flux line lattice in the channels.

with the tangent to the linear section in the real part of the AC susceptibility measured at low AC field amplitude. The use of this criterion in the sample containing a channel structure has to take into account the existence of a double-step transition. One may thus define the two lines S_1 and S_2 as two different transitions to the normal state. A striking fact is the coincidence between the S_1 line and $H_{c2}(T)$ measured in non-irradiated samples. It points out that the double-step transition corresponds to the contribution of two different fractions of the irradiated sample: the non-irradiated channels, where the transition is the same as in pristine samples, and the irradiated parts with a higher value of H_{c2}. This can be due to a possible strong perturbation of the charge–density wave caused by the irradiation damages. The disappearance of the peak-effect in the critical-current density observed in pristine samples, also results from the irradiation [15].

A satisfactory interpretation of the double-step transition is thus the following: the sample is composed of two phases, each of them undergoing the superconducting transition at different fields $H_{c2}(T)$. The phase characterised by the absence of columnar defects has a T_c of 7.13 K, in good agreement with the data obtained on non-irradiated samples [28], whereas the irradiated fraction of the sample has a higher critical temperature, $T_c = 7.27$ K. It is worth mentioning that the intercept of the linear part in the resistivity data and the normal-state line also falls on the line S_1 at low DC fields. The difference between the behaviours of both fractions of the sample decreases as the DC field is increased (or the temperature lowered); this difference disappears at DC fields close to 0.6 T, where the influence of the irradiated part of the sample becomes undetectable, and the two peaks in χ'' merge. The same kind of behaviour is visible in the $\chi''(H)$ measurements performed at different AC field amplitudes (Fig. 3): both peaks move to lower DC field, the second peak showing a more marked AC field dependence than the first one, as it moves towards that at lower DC field upon increasing the AC amplitude. This behaviour is opposite to that of granular (polycrystalline) samples, in which an increase of the applied (AC or DC) magnetic field produces an increasing splitting between the so-called intergranular and intragranular peaks [29].

In fact one has to consider the morphology of the sample: a succession of parallel non-irradiated channels separated by high-pinning stripes. The vortex ensemble in the non-irradiated channels can only be set into motion when the driving force is large enough to overcome the shear stress at the channel edges, or if a structural transition of the vortex ensemble strongly modifies the shear modulus, like e.g. the melting transition, where the shear modulus C_{66} is supposed to rapidly fall to zero. The weak amplitude dependence of the first peak (the peak at low DC field or low temperature, see Fig. 3) suggests such a scenario. In the case of bulk pinning irreversibility, a peak is observed when the AC field amplitude matches a characteristic value, which is directly proportional to the critical current density. A weak amplitude dependence of the peak indicates that this characteristic value varies very rapidly over a small temperature range, and hence, we conclude that the drop of the critical current density is sharp, as expected at the melting transition [2]. Therefore, the shear from the channel edges, associated with the melting transition, occurs simultaneously as the drop of j_c.

The second peak observed at higher DC field (or temperature) can be ascribed to the depinning from the columnar defects, corresponding to the kink in the resistivity as well. This is consistent with the more pronounced amplitude dependence which, in the framework of the critical-state model, is due to a less abrupt decrease of j_c, as depinning from the columnar defects in the Bose-glass state is not a first-order transition in the thermodynamic sense (see the case of Bi-2212 Ref. [19]). Note that the Bose-glass description of the vortex state has been shown to be valid only at fields lower than approximately half the dose-equivalent field in Bi-2212. This is in good agreement with the disappearance of both the kink in resistivity and the second peak in AC susceptibility at fields around 0.6 T (half the matching field is 0.5 T in our case), as these features have been ascribed to the high pinning by the columnar defects in the stripes between the channels.

A consideration of the I–V curves supports this interpretation, as linearity is only observed above the R_{kink} line, i.e. when the whole vortex ensemble is depinned in the entire sample. The non-linear behaviour observed in the intermediate region between

the R_{kink} and the R_0 line is due to pinning by the columnar defects stripes separating the channels, while the vortices already move freely in the channels. Below the R_0 line, a current density j_s can be clearly defined from the I–V curves. Below this current there is no detected motion of flux lines in the channels and in the irradiated regions (I–V curve measured at $T = 6.5$ K and $H = 302$ mT in Fig. 5). A comparison can be done between the value of the critical current and the theoretical estimate (within a continuum approximation of the flux line lattice) of the shear current density [23] J_s. By taking the values of the in-plane Ginzburg–Landau penetration depth $\lambda_{ab}(0) = 2000$ Å, $T = 6.5$ K, $T_c = 7.13$ K for the non-irradiated portion, and $J_s = 1.23 \cdot 10^6$ A/m^2, and using the Expressions (1) and (2), one finds for the constant A the value 0.0255, which is close to the theoretical value $1/30$, and to the value 0.047 found in the Refs. [21–23,30].

One of the main differences between the results presented in this paper and the experiment carried out on 2D flux lines in amorphous Nb_3Ge patterned with a channel structure of high pinning material NbN [20], is that the vortices can be depinned from the columnar defects, whereas they rigorously remain pinned by the NbN layer up to a temperature above T_c in Nb_3Ge. Therefore, it is not possible to extract the shear viscosity following the procedure described in Ref. [20], because both the shear and the depinning contributions are mixed. If this were not the case, the I–V curves should consist of two linear portions separated by a non-linear section in the area comprised between the R_0 and the R_{kink} line. The linear section at low currents would correspond to the flow in the channels, while the other linear part at high currents to the flux flow over the entire sample. The non-linear section at intermediate currents could then be ascribed to depinning from the columnar defects.

5. Conclusion

Transport measurements have been carried out on 2H-$NbSe_2$ samples consisting of non-irradiated channels separated by stripes with columnar defects. The experimental configuration is such that the vortices are constrained to flow within the channels. The presence of a double-step transition in AC susceptibility measurements at low AC field amplitude shows that the sample is characterised by two critical temperatures each of them corresponding to the irradiated and non-irradiated portions of the sample, respectively. Below H_{c2}, two lines can be constructed in the H–T diagram from the resistivity measurements. At low temperatures and low fields the vortex ensemble is pinned by the columnar defects, and in the channels the weak-pinning centres and the shear force at the edges prevents the vortices from flowing. As temperature is increased, the onset of flow in the channels takes place when the lattice melts as a result of the vanishing shear modulus. Upon further increasing the temperature, a point is reached where the vortices depin from the columnar defects, resulting in an uniform flux flow over the entire sample. An important distinction between the results presented in this paper and similar experiments carried out on low-T_c's patterned with a high pinning channel structure, is the possibility for the vortices to depin from the columnar defects. Nevertheless, the value of the constant A has been found to be in good agreement with previously reported theoretical and experimental values.

Acknowledgements

The assistance of M. Konczykowski for the irradiation process is gratefully acknowledged. We would like to thank S. Ramakrishnan, J. Aarts and R.J. Drost for valuable discussions and a critical reading of the manuscript. We are also grateful to L.A. Angurel for providing us with some of his results.

References

[1] D.R. Nelson, Phys. Rev. Lett. 60 (1988) 1973.
[2] G. Blatter, M.V. Feigel'man, V.B. Geshkenbein, A.I. Larkin, V.M. Vinokur, Rev. Mod. Phys. 66 (1994) 1125.
[3] E.H. Brandt, Rep. Prog. Phys. 58 (1995) 465.
[4] H. Pastoriza, M.F. Goffman, A. Arribére, F. de la Cruz, Phys. Rev. Lett. 72 (1994) 2951.
[5] E. Zeldov, E. Majer, M. Konczykowski, V.B. Geshkenbein, V.M. Vinokur, H. Shtrikman, Nature (London) 375 (1995) 373.

[6] A.K. Pradhan, S. Shibata, T. Machi, K. Nakao, N. Koshizuka, Physica C 315 (1999) 159, and references therein.
[7] R. Cubitt, E.M. Forgan, G. Yang, S.L. Lee, D.Mck. Paul, H.A. Mook, M. Yethhiraj, P.H. Kes, T.W. Li, A.A. Menovsky, Z. Tarnawski, K. Mortensen, Nature (London) 365 (1993) 407.
[8] S. Lee, P. Zimmermann, H. Keller, M. Warden, I.M. Savic, R. Schuwecker, D. Zech, R. Cubitt, E.M. Forgan, P.H. Kes, T.W. Li, A.A. Menovsky, Z. Tarnawski, Phys. Rev. Lett. 71 (1993) 3862.
[9] K. Harada, T. Matsuda, H. Kasai, J.E. Bonevich, T. Yoshida, U. Kawabe, A. Tonomura, Phys. Rev. Lett. 71 (1993) 3371.
[10] P. Koorevaar, J. Aarts, P. Berghuis, P.H. Kes, Phys. Rev. B 42 (1990) 1004.
[11] K. Ghosh, S. Ramakrishnan, A.K. Grover, G.I. Menon, G. Chandra, T.V. Chandrasekhar Rao, G. Ravikumar, P.K. Mishra, V.C. Sahni, C.V. Tomy, G. Balakrishnan, D. Mck Paul, S. Bhattacharya, Phys. Rev. Lett. 76 (1996) 4600.
[12] A.I. Larkin, Yu.N. Ovchinnikov, J. Low Temp. Phys. 34 (1976) 409.
[13] S. Ramakrishnan, K. Ghosh, A.K. Grover, G.I. Menon, T.V. Chandrasekhar Rao, G. Ravikumar, P.K. Mishra, V.C. Sahni, C.V. Tomy, G. Balakrishnan, D. Mck Paul, S. Bhattacharya, Physica C 256 (1996) 119.
[14] S. Bhattacharya, M.J. Higgins, T.V. Ramakrishnan, Phys. Rev. Lett. 73 (1994) 9699.
[15] M. Chung, Y.-K. Kuo, Z. Xu, L.E. DeLong, J.W. Brill, R.C. Budhani, Phys. Rev. B 50 (1994) 1329.
[16] L. Civale, A.D. Marwick, T.K. Worthington, M.A. Kirk, J.R. Krusin-Elbaum, Y. Sun, J.R. Clem, F. Holtzberg, Phys. Rev. Lett. 67 (1991) 648.
[17] M. Konczykowski, F. Rullier-Albenque, E.R. Yacoby, A. Shaulov, Y. Yeshurun, P. Lejay, Phys. Rev. B 44 (1991) 7167.
[18] W. Gerhäueser, G. Ries, H.W. Neumüller, W. Schmidt, O. Eibl, G. Saemann-Ischenko, S. Klaumünzer, Phys. Rev. Lett. 68 (1992) 879.
[19] C.J. van der Beek, M. Konczykowski, V.M. Vinokur, G.W. Crabtree, T.W. Li, P.H. Kes, Phys. Rev. B 51 (1995) 15492.
[20] A. Pruymboom, P.H. Kes, E. van der Drift, S. Radelaar, Phys. Rev. Lett. 60 (1988) 1430.
[21] R. Schmucker, Philos. Mag. 35 (1977) 431.
[22] A. Seeger, in: Handbuch Physik vol. 7 Springer, Berlin, 1958, p. 2.
[23] M.H. Theunissen, E. Van der Drift, P.H. Kes, Phys. Rev. Lett. 77 (1996) 159.
[24] H. Pastoriza, P.H. Kes, Phys. Rev. Lett. 75 (1995) 3525.
[25] C.J. van der Beek, M.V. Indenbom, G. D'Anna, W. Benoit, Physica C 258 (1996) 105.
[26] G. D'Anna, M.-O. André, W. Benoit, E. Rodriguez, D.S. Rodriguez, J. Luzuriaga, J.V. Wasczak, Physica C 218 (1993) 238.
[27] M. Marchevsky, L.A. Gurevich, P.H. Kes, J. Aarts, Phys. Rev. Lett. 75 (1995) 2400.
[28] L.A. Angurel, F. Amin, M. Polichetti, J. Aarts, P.H. Kes, Phys. Rev. B 56 (1997) 3425.
[29] in: R.A. Hein, T.L. Francavilla, D.H. Liebenberg (Eds.), Magnetic Susceptibility of Superconductors and Other Spin Systems, Plenum, New York, 1991.
[30] R. Wördenweber, P.H. Kes, C.C. Tsuei, Phys. Rev. B 33 (1986) 3172.